

Design and verification of an electrostatic MEMS simulator

V. Székely**, G. Bognár**, M. Rencz*, F. Ciontu***, B. Charlot***, B. Courtois***

*MicReD Ltd, Hungary

rencz@micred.com

Tel: +361 463 2727, Fax: +36 1 463 2973

** Budapest University of Technology and Economics, Hungary

***TIMA Laboratory, Grenoble, France

ABSTRACT

In this paper we introduce algorithmic extensions to thermal simulators in order to fit them also for electrostatic simulation. The advantage is the simplicity and the speed of this kind of simulation. We present the algorithm of calculating the forces in details. The algorithm is verified with results measured on a MEMS structure. An electrostatic comb drive was designed, fabricated and measured. The comparisons of the measured and simulated results demonstrate the applicability of the simulation method in addition to presenting a way for the electrostatic characterization of comb drives by measurements.

Keywords: electrostatic simulation, calculation of forces, comb drives, MEMS simulation, MEMS characterization.

1 INTRODUCTION

The SUNRED algorithm has been developed originally for the fast and user friendly thermal simulation of microelectronic structures with finite difference method (FDM). [1],[2],[3]. Since the same type of differential equation, the so-called Poisson equation, gives the description of electrostatic problems, basically the same solvers can be used for the solution of the two problems. The $T(x,y,z)$ stationary thermal field is described by the differential equation of

$$\operatorname{div}(\lambda \operatorname{grad} T) = -p \quad (1)$$

where λ is the space-dependent thermal conductivity and p is the dissipation density. The static electric field satisfies a very similar equation:

$$\operatorname{div}(\varepsilon \operatorname{grad} V) = -\rho \quad (2)$$

where V is the potential, ε is the dielectric permittivity and ρ is the charge density. The applicable rules of analogy are the followings: voltage corresponds to temperature, permittivity corresponds to heat conductivity and charge density corresponds to dissipation density. By the application of these rules, thermal solvers become suitable to solve static electric fields as well.

A new problem is encountered however in the electrostatic simulation of MEMS structures, having no thermal field analogy. This is the calculation of the forces acting on

the different pieces of matter, present in an electrostatic scenario. Possible solutions for this problem are shown in the first part of the paper. The second part of the paper gives the verification of the presented algorithm by comparing the simulated results with results measured on a realized comb drive.

2 CALCULATION OF ELECTROSTATIC FORCES

In the frequently applied solution forces are calculated from the energy balance. A small ds displacement of the piece of matter is supposed along an arbitrary s direction, and the resulted changes in the capacitances are calculated. For two electrodes, that is, for one capacitance this results in the well-known relationship of

$$F = \frac{1}{2} V^2 \frac{dC}{ds} \quad , \quad (3)$$

where C is the capacitance between the two electrodes and V is their voltage difference. If the directions are the $i = 1 \dots 3$ coordinates the Cartesian components of the force vector are obtained as follows:

$$F_i = \frac{1}{2} V^2 \frac{dC}{dx_i} \quad . \quad (4)$$

In case of multiple electrodes, the force can be calculated as the sum of the forces calculated from the partial capacitances:

$$F_i = \frac{1}{2} \sum_{m=2}^N \sum_{n=1}^{m-1} (V_m - V_n)^2 \frac{dC_{mn}}{dx_i} + \frac{1}{2} \sum_{m=1}^N V_m^2 \frac{dC_{m\infty}}{dx_i} \quad , \quad (5)$$

where N is the number of electrodes, V_m is the voltage of the m -th electrode, C_{mn} is the partial capacitance between the m -th and n -th electrodes, $C_{m\infty}$ is the partial capacitance between the m -th electrode and the infinitely distant point of the field.

The partial capacitances between the electrodes may be calculated easily. Forcing unit voltage on one electrode while zero voltage is forced to all the others the calculation of the charges on the electrodes results in the corresponding column of the matrix equation of

$$Q_m = \sum_{n=1}^N a_{mn} V_n \quad . \quad (6)$$

From the a_{mn} coefficients the capacitances may be calculated as follows:

$$C_{mn} = -a_{mn} \quad m \neq n \quad , \quad C_{m\infty} = \sum_{n=1}^N a_{mn} \quad (7)$$

The main difficulties encountered in the practical implementation are as follows:

- Calculation of the a_{mn} matrix needs N runs. Calculation of the derivatives needs the displacement of the examined electrode in one direction with Δx_i and a new analysis. Calculating the three components of the forces on each electrode requires a large number of runs.
- Displacing an electrode is not easy if the description was given on a non-equidistant grid.
- Calculating the forces acting on the pieces of dielectrics, according to the above-described methodology requires a further large number of runs.

For all these reason in the SUNRED program a different approach is used for the calculation of the forces, as follows.

With the help of Eq.(2) the distribution of the electrical field may be calculated for complex electrode-dielectric arrangements. This field is originated from the positive and negative charges influenced by the opposed surfaces. The permittivity of the dielectric materials results in the rearrangement of the electrostatic dipoles in them, yielding also in surface charge layers. This is presented in Figure 1.

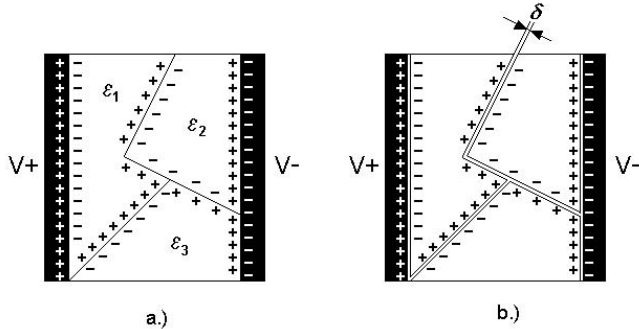


Figure 1. Dipole layers separating the surfaces of contacting materials

Knowing the field distribution the surface charges may be calculated with the Gauss law of electrostatics. If both the field and charge distributions are known the forces may be calculated. With this method the forces effecting all electrodes and dielectrics may be calculated by one simulation only.

During the simulation a $\delta \rightarrow 0$ air-gap is supposed between all the different pieces of matter, see Figure 1b. With this condition each piece of matter may be investigated individually. Let us examine, the electro static field components on the surface of a matter of ϵ_r relative permittivity, see Figure 2.

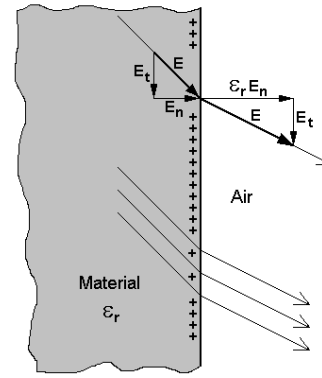


Figure 2. Field components at the surface of a matter of ϵ_r permittivity

On the left and right hand side of the surface the E_t tangential field components equal, in order to match the potentials of the Material and Air-sides. The E_n normal direction component of the field strength shows a difference depending on the permittivities. From this difference the surface charge may be calculated as follows:

$$Q = e_0 (E_n - e_r E_n) A \quad , \quad (8)$$

where A is the area of the investigated elementary surface region, e_0 is the permittivity of the vacuum.

The mean value of the normal component of the field strength can be written as follows:

$$\bar{E}_n = \frac{1}{2} (E_n + e_r E_n) = E_n \frac{1+e_r}{2} \quad . \quad (9)$$

Exploiting the fact that the electrostatic force can be calculated as the product of the field strength and the charge, the normal and tangential components of the force (F_n and F_t) acting to the investigated area can be written as follows:

$$\begin{aligned} F_n &= Q \bar{E}_n = \epsilon_0 A E_n^2 (1 - \epsilon_r^2) / 2 \\ F_t &= Q E_t = \epsilon_0 A E_n E_t (1 - \epsilon_r) \end{aligned} \quad (10)$$

Using the mean value of \bar{E}_n in Eq. (10) seems to be an approximation and a potential source of inaccuracies. The rigorous derivation provides however the same result, as long as the thickness of the surface charge layer is negligible compared to the radius of the surface curvature.

If we wish to implement any of the above presented methods of calculating the electrostatic forces in a program that is solving Eq.2 with finite difference method, errors have to be expected as a result of the finite mesh. The error are pronounced at the corners of the electrodes, where the distribution of the field shows strong inhomogeneity. We investigated the strength of this error by runs with different mesh sizes. The examined 2D structure is shown in Figure 3. Exploiting the symmetries a $1/4$ -th of the structure was simulated. The capacitances and the forces were calculated with various grid densities. The results are presented in Table 1 in relative units, in the percentage of the data obtained with the finest grid structure.

Table 1

M (mesh point)	Capacitance	Force
4	0.9535	0.7848
8	0.9807	0.8504
16	0.9921	0.8958
32	0.9969	0.9289
64	0.9988	0.9539
128	0.9996	0.9731
256	0.9999	0.9881
512	1	1

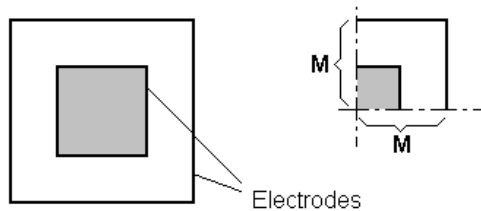


Figure 3. The structure examined with different mesh point numbers

We can conclude that the calculation of the capacitances may be correct even in the case of a rough mesh, but the calculation of the forces according to Eq.(10) is rather sensitive to the mesh fineness.

3 VERIFICATION USING A REALIZED COMBDRIVE

In the TIMA Laboratory several combdrive structures have been realized, using the MemsCap PolyMUMPs technology. One of them has been used to verify the results calculated by the SUNRED engine. The micro-photograph of the investigated structure is shown in Figure 4.

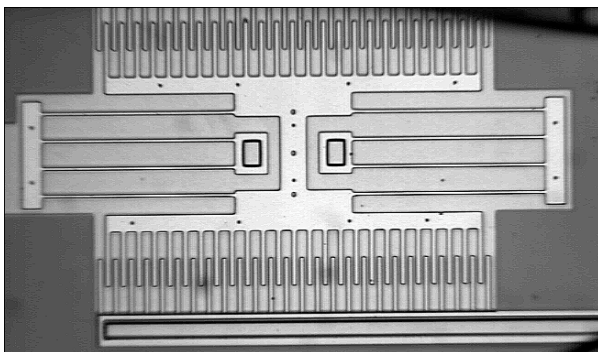


Figure 4. The micro-photograph of the investigated comb drive

Both the fixed and the mobile parts of the comb structure are made of the 2nd poly-silicon layer. The main sizes of the structure are as follows. The thickness of the poly is 2 μm. The teeth are 40 μm long and 3 μm wide, the air gap is 3 μm as well. The 8 hanging springs are 150 μm long and 2 μm wide each. The moving part is electrically grounded and the fixed combs are excited alternately by a

voltage of 50-150 V. Beneath the whole structure a conducting layer is present, made of the 1st poly-silicon. This layer is grounded. The gap between the 1st and the 2nd poly is 2 μm.

The following data have been measured on the structure. The most important static characteristic is the voltage/displacement function, which has to be quadratic. The measured results are shown in Figure 5, in quadratic voltage and linear displacement scales. The line fitted to the measured points shows that, the structure correctly obeys the quadratic law. The fitted displacement function is

$$d = d_0 \cdot V^2 = 1.35 \cdot 10^{-4} V^2 \quad [\mu\text{m}] = 1.35 \cdot 10^{-10} \cdot V^2 \quad [\text{m}]$$

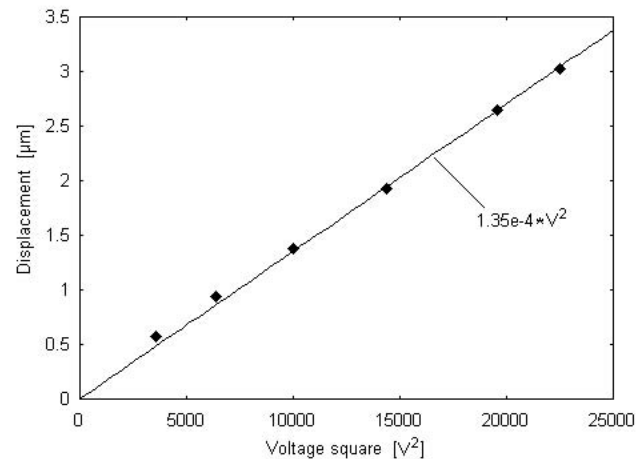


Figure 5. The measured voltage-displacement function (dots: measured data, line: quadratic approximation)

The most important dynamic characteristic of the combdrive is the f_0 resonance frequency. The measured value of f_0 is 20 kHz.

The above-presented data allow the calculation of the spring constant of the suspension in two ways. The first way is to use the geometrical data and the Young's modulus of the matter. The compliance for one arm of the spring can be calculated as follows:

$$S = \frac{l^3}{12EI} = \frac{(1.5 \cdot 10^{-4})^3}{12 \cdot 1.4 \cdot 10^{11} \cdot 1.33 \cdot 10^{-24}} = 1.51 \text{ m/N} \quad (11)$$

where $E \cong 140$ GPa is considered for the poly-silicon, (130-150 GPa was reported for doped layers in [4]), and $I = 1.33 \cdot 10^{-24} \text{ m}^4$ is the momentum of inertia for the $2 \times 2 \mu\text{m}$ cross-section of the spring. Taking into account that the springs are connected partly in parallel partly in series we obtain

$$S = 0.76 \text{ m/N} \quad (12)$$

for the overall spring compliance.¹

The second way to determine the spring constant is to derive it from the resonance frequency. The overall mass of

¹ In order to avoid confusion with the C capacitance, in this paper we use the notation of S for the spring compliance.

the moving part can be calculated from the geometrical data and the density of the silicon. This calculation leads to $m = 8.53 \cdot 10^{-11}$ kg. The frequency is given by

$$f_0 = \frac{1}{2\pi\sqrt{mS}} \quad (13)$$

From this equation the following value is obtained for the S spring compliance:

$$S = \frac{1}{m(2\pi f_0)^2} = \frac{1}{8.41 \cdot 10^{-11} (12.56 \cdot 10^4)^2} = 0.753 \text{ m/N} \quad (14)$$

This value is in good agreement with (12).

The electrostatic force can be calculated now as

$$F = \frac{d}{S} = \frac{d_0}{S} V^2 = F_0 V^2, \quad (15)$$

where

$$F_0 = \frac{d_0}{S} = \frac{1.35 \cdot 10^{-10}}{0.76} = 1.78 \cdot 10^{-10} \text{ N/V}^2. \quad (16)$$

This F_0 actuator-constant has to be calculated by the SUNRED engine in order to verify the correctness of the calculation of the electrostatic forces.

During the simulation a suitable part of the comb structure was investigated. The modeled part is shown in Figure 6. In order to correctly model the effect of the adjacent teeth the comb structure was cut in its symmetry planes.

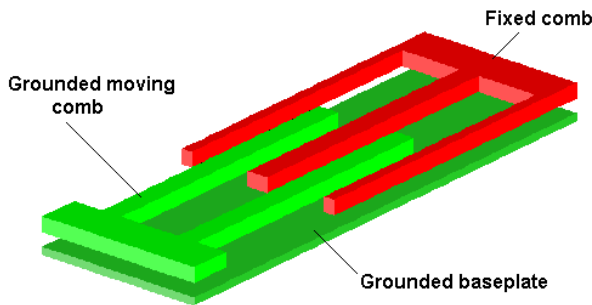


Figure 6. The modeled part of the comb structure

First we calculate the force using the energy balance method. The partial capacitances were calculated for two positions of the moving comb. Eq. (5) has been used for the calculation of the force. The result is

$$F_0 = 1.4 \cdot 10^{-10} \text{ N/V}^2, \quad (17)$$

which is close to the measured actuator-constant (Eq.(16)). The error of about 20% may be originated from the differences between the nominal and real geometric sizes and the ambiguities of material parameters.

In the second run the actuator-constant has been calculated using Eq.(10). This resulted in

$$F_0 = 1.05 \cdot 10^{-10} \text{ N/V}^2. \quad (18)$$

The difference between this and the result of Eq.(17) can be explained by the limited mesh resolution, see Table 1.

During the simulation some interesting second-order effects have been observed, which are instructive for further

combedrive designs. The first one is that the grounded baseplate destroys the effectiveness of the electrostatic actuation. The same structure but without the baseplate produces $F_0 = 2.45 \cdot 10^{-10} \text{ N/V}^2$. If the baseplate is present, but the gap between poly1 and poly2 is $2.5 \mu\text{m}$ instead of $2 \mu\text{m}$, F_0 increases with 15 %.

A further interesting result is that in the structure of Figure 4 the simulation shows an off-plane force as well, beyond the expected in-plane force. This off-plane force tends to push out the teeth of the moving electrode upwards, in the vertical direction. The calculated forces for 100V excitation are:

$$F_{\text{in-plane}} = 0.904 \cdot 10^{-6} \text{ N}, \quad F_{\text{off-plane}} = 3.92 \cdot 10^{-6} \text{ N}.$$

This result was so surprising that we considered indispensable to verify it. In fact, a slight rise of the moving comb was observed if the fixed comb was excited. We were able to measure the amount of this rise only for strong excitation, the value of the rise was $1.3 \mu\text{m}$ for 150 V excitation. Accepting this fact, the F_0 values of Eqs. (17) and (18) were calculated with the appropriate vertical offset of the moving comb position.

4 CONCLUSIONS

As the presented case study shows, the simulated results fit acceptably with the results that we have measured on a realized MEMS structure. Both presented methods are suitable to calculate the electrostatic forces. The first presented method gives more accurate results, but the quickly obtainable results of the second presented method make it a good solution for fast orienting calculations in FDM solvers.

5 ACKNOWLEDGMENTS

This work was partially supported by the PROFIT IST-1999-12529 Project of the EU, and the 2/018/NKFP-2001 INFOTERM Projects of the Hungarian Government.

REFERENCES

- [1] V. Székely and M. Rencz: "Fast field solvers for thermal and electrostatic analysis", *DATE Proceedings*, Feb. 23-26 Paris, France, pp. 518-523, 1998
- [2] A. Páhi, V Székely, M. Rosenthal, M. Rencz: "3D extension of the SUNRED field solver", *4th THERMINIC Workshop*, 27-29 September 1998, Cannes, France, pp. 185-190
- [3] V. Székely, M. Rencz, A. Poppe and G. Farkas: "User friendly tools for the thermal simulation and modelling of electronic subsystems", *3^d Int. Conf. on Benefiting from Thermal and Mechanical Simulation in (Micro)-Electronics, EuroSIME 2002*, 15-17 April 2002, Paris, France, pp. 254-261
- [4] A. Nathan, H. Baltes: *Microtransducer CAD*, Springer-Verlag, Wien, New York, 1999
- [5] S. D. Senturia: *Microsystem Design*, Kluwer Academic Publishers, Boston, 2001